Published in final edited form as:

Obesity (Silver Spring). 2020 June ; 28(6): 1075–1085. doi:10.1002/oby.22763.

Weight loss and concomitant adipose autophagy in methionine-restricted obese mice is not dependent on adiponectin or FGF21

Diana Cooke[1], **Dwight Mattocks**[1], **Sailendra N. Nichenametla**[1], **Rea P. Anunciado-Koza**[2], **Robert A. Koza**[2], **Gene P. Ables**[1]

[1]Orentreich Foundation for the Advancement of Science, Inc., Cold Spring-on-Hudson, NY, USA

[2]Maine Medical Center Research Institute, Scarborough, Maine, USA

Abstract

Objective -—Identifying novel approaches to combat obesity is important to improve healthspan. We hypothesize that methionine restriction (MR) will induce weight loss in obese mice by reducing adipose tissue mass due to increased energy expenditure (EE) and reprogramming of adipose tissue homeostasis. We also test the roles of adiponectin (ADIPOQ) and fibroblast growth factor 21 (FGF21) during weight loss in MR mice.

Methods -—We used diet-induced obese (DIO) male C57BL/6J (WT), *Adipoq*-deficient (*Adipoq*-KO), *Fgf21*-KO, and *Adipoq-Fgf21* double-knockout (AF-dKO) mice. Following a switch to high-fat control (DIO-CF, 60% fat/0.86% methionine) or MR (DIO-MR, 60% fat/0.12% methionine) diets, physiological parameters were measured, and inguinal and perigonadal adipose tissue were examined.

Results -—Obese mice subjected to MR showed loss of body weight and adiposity, increased EE, and improved glucose tolerance that was independent of the actions of ADIPOQ and FGF21. MR induced reduction of circulating lipids, glucose, insulin, leptin, and IGF1 and increased β-hydroxybutyrate, ADIPOQ, and FGF21 concentrations. In fat, MR upregulated protein levels of ATGL, AIF, LAMP1/2, ATG5, Beclin1, and LC3BI/II.

Conclusion -—MR reduction of adipose tissue mass in obese mice is associated with elevated lipolysis, apoptosis, and autophagy and occurs independently of the actions of ADIPOQ and FGF21.

Keywords

methionine restriction; weight loss; adiponectin; FGF21; obesity

CONTACT INFO: Gene P. Ables, Ph.D., Orentreich Foundation for the Advancement of Science, Inc., 855 Route 301, Cold Spring, NY 10516, Phone: (845) 265-4200, Fax: (845) 265-4211, gables@orentreich.org.

AUTHOR CONTRIBUTIONS: DC, DM, RA-K, RK, SN, and GA participated in the animal experiments and data analysis. DC and DM conducted genotyping, gene, and protein expression experiments. RA-K and RK conducted calorimetry studies. GA designed the experiments and wrote the manuscript. All authors have read and approved the manuscript.

DISCLOSURE: The authors declared no conflict of interest.

INTRODUCTION

Obesity increases the risk for metabolic diseases and cancer (1,2). Although obesity prevention is the best strategy, in most cases the obese condition already exists; therefore, weight loss is necessary to attenuate morbidity. In rodents, methionine restriction (MR) prevents adipose tissue accumulation due to a futile lipid cycle (3). Additionally, MR increases energy expenditure (EE) and induces beige adipose tissue formation in rodents compared to controls (4,5). However, the ability of MR to reverse obesity has not yet been thoroughly examined. In this study, we use mice fed a high-fat diet (HFD) for at least 8 weeks to induce obesity before switching them to either a control (DIO-CF) or MR (DIO-MR) diet. We hypothesize that MR will induce weight loss in DIO mice by reducing adipose tissue mass due to increased EE and an enhanced futile lipid cycle. We also test the roles of adiponectin (ADIPOQ) and fibroblast growth factor 21 (FGF21) in eliciting weight loss in obese mice undergoing MR.

The roles of ADIPOQ and FGF21 during MR under obese conditions have not been fully examined. Circulating ADIPOQ and FGF21 are consistently elevated during MR, (4,6) suggesting that these two hormones are required for the beneficial effects of MR. While initial studies demonstrated that ADIPOQ is mainly secreted from fat (7) and FGF21 from the liver (8), recent findings indicate that both hormones have pleiotropic targets and are secreted from multiple organs (9,10). Individually, ADIPOQ and FGF21 have similar actions on glucose metabolism and energy balance. Either ADIPOQ or FGF21 promotes insulin sensitivity associated with obesity (7,11). Additionally, independent studies have demonstrated that both ADIPOQ and FGF21 act on the central nervous system to induce weight loss in obese mice (12,13). Importantly, during cold challenge, both *Adipoq*-KO and *Fgf21*-KO mice exhibit lower body temperature with reduced BAT thermogenesis and beige adipose tissue formation (14,15). Interestingly, separate studies have shown that, during MR, *Adipoq*-KO and *Fgf21*-KO mice lose body weight and adiposity similarly to WT mice, suggesting that the 2 hormones are not necessary to maintain energy balance (16,17). However, these studies did not demonstrate whether the lack of effect of one hormone during MR is due to compensation by the other hormone. Nevertheless, several studies have demonstrated that the ADIPOQ–FGF21 axis establishes crosstalk between liver and adipose tissue in helping to maintain glucose homeostasis and energy balance (18,19). Therefore, to clearly define the roles of ADIPOQ and FGF21 during MR, we created mice that lacked both hormones.

Rodents undergoing MR resist adipose tissue accumulation due to increased lipogenesis and lipolysis; this occurs via activation of 11β-hydroxysteroid dehydrogenase 1, adipocyte triglyceride lipase (ATGL), and acetyl-coenzyme A carboxylase enzymes (3). MR also induces mitochondrial biogenesis in inguinal white adipose tissue (iWAT) of rats and mice (20). Finally, MR rodents display enhanced EE with the appearance of multilocular adipocytes and upregulation of UCP1 expression in iWAT (20). However, these findings are from experiments conducted in rodents that were not obese before beginning MR.

Our studies indicate that MR promotes weight loss in obese mice independent of the actions of ADIPOQ and FGF21. Interestingly, adipose tissue lipolysis and lipogenesis during MR

are variably affected by the hormones. Our data also show a depot-specific coordinated response by obese mice during MR that is associated with a synchronized mechanism that regulates adipose tissue homeostasis.

METHODS

Animal Care.

All studies were approved by the Institutional Animal Care and Use Committees of the Orentreich Foundation for the Advancement of Science, Inc. (Permit Number: 0511MB) and the Maine Medical Center Research Institute. Male C57BL/6J mice (WT, #000664) and a breeder pair of ADIPOQ-knockout mice (*Adipoq*-KO, *Adipoq*^{tm1Chan}, #008195) were purchased from The Jackson Laboratory (Bar Harbor, Maine). FGF21 knockout (*Fgf21*-KO) mice were provided by Dr. Steven Kliewer (University of Texas Southwestern Medical Center). *Adipoq-Fgf21* double-knockout (AF-dKO) mice were generated in our facility by crossing *Adipoq*-KO and *Fgf21*-KO mice and genotyped using standard protocols (21,22). Mice were singly housed, maintained at 20 ± 2°C, 50 ± 10% relative humidity, a 12 h light: 12 h dark photoperiod with *ad libitum* food and water. To induce obesity, 8-week-old mice were fed HFD (60% kcal fat, D12492, Research Diets, New Brunswick, New Jersey) for at least 8 weeks. All mice were weight-matched and divided into 2 groups (n = 5–8/group) that were fed either a control (DIO-CF, 60% fat/0.86% methionine, Research Diets A14032002) or an MR (DIO-MR 60% fat/0.12% methionine, Research Diets A14032001, Table S1) diet for 8 weeks. *Fgf21*-KO mice were fed for 12 weeks. Body weight and food consumption were measured twice weekly. On the day of sacrifice, mice were fasted for 4 hours, euthanized, and dissected for organ collection. Plasma was collected, and perigonadal (pgWAT), inguinal (iWAT), and interscapular brown (BAT) adipose depots were collected, snap-frozen, and stored at −80°C until processed.

Animal Measurements.

Fat and lean masses (g) were measured using a PIXImus dual-energy X-ray absorptiometry (DEXA) instrument as described previously (6). Body composition of mice used for indirect calorimetry studies was measured by nuclear magnetic resonance (NMR) using a Minispec LF-50 BCA-Analyzer (Bruker Corp., Billerica, Massachusetts) at Maine Medical Center Research Institute (MMCRI), Scarborough, Maine. Indirect calorimetry using the Promethion Metabolic Cage System (Sable Systems, Las Vegas, Nevada) was conducted at MMCRI. Briefly, 30 7-week-old male C57BL/6J mice were singly housed and fed chow (2018 Teklad Global 18% Protein Rodent Diet, Harlan, Indianapolis, Indiana) for 1 week. At 8 weeks of age, mice were switched to HFD until bodyweights of most of the mice reached 36–44 grams. After 11 weeks of HFD-feeding, diet was switched to DIO-CF for 8 weeks, at which time the mice were placed in metabolic chambers. After 1 week of acclimatization in the chambers, mice were divided into 2 weight-matched groups (n = 8/group) and fed either DIO-CF or DIO-MR. EE and respiratory quotient (RQ) were measured for 6 days. Mice were then euthanized, and tissues were harvested for analyses.

Glucose Metabolism Experiments.

Glucose metabolism experiments were conducted as described previously (6). Briefly, intraperitoneal glucose tolerance tests (GTT) using 10% glucose at 1 mg/kg dose were conducted 4 weeks after diet switch to either DIO-CF or -MR for all mouse cohorts. AF-dKO DIO mice underwent a pyruvate tolerance test (PTT) using 20% sodium pyruvate at 1 g/kg dose to estimate hepatic gluconeogenesis at 5 weeks, and insulin tolerance tests (ITT) using 100 mU of insulin at 1 U/kg dose at 7 weeks after the diet switch. For each test, blood glucose was measured from a tail nick before injection (time 0) and at 15, 30, 60, 90, and 120 min after injection using a handheld Abbott® Freestyle glucometer and test strips.

Blood Biochemical Tests.

ELISA kits were used to measure insulin (ALPCO Diagnostics, Salem, New Hampshire), leptin, IGF-1, ADIPOQ (R&D Systems, Minneapolis, Minnesota), and FGF21 (Millipore Corp., Billerica, Massachusetts). Colorimetric assays were used to determine plasma triglycerides (TG), total cholesterol (TC) (Thermo Scientific, Middletown, Virginia), and ß-hydroxybutyrate (BHB, Cayman Chemical, Ann Arbor, Michigan).

Histological Analysis.

For hematoxylin and eosin (H & E) staining, adipose tissue samples were fixed in 10% formalin solution (Thermo Scientific), paraffin-embedded, and sectioned at 5 μm. For adipocyte sizing in pgWAT, we used NIS-Elements AR 5.02.01 software (Nikon, Tokyo, Japan). Fifteen intact adipocytes per section of pgWAT from each animal were randomly selected under 20× magnification, and area was measured using polygon function.

Gene Expression Analysis.

Gene expression analysis in adipose tissue by quantitative real-time PCR (qPCR) was conducted as previously described (6). Briefly, 1 μg of RNA was reverse transcribed to cDNA using High-Capacity cDNA Reverse Transcription Kit (Life Technologies, Carlsbad, California), and qPCR was conducted in a StepOnePlus Real-Time PCR System using TaqMan primer-probe sets (Life Technologies) (Table S2). Gene expression was assessed by comparative CT (ΔΔCT) method using β-actin as reference.

Western Blot Analysis.

Adipose tissues were homogenized in ice-cold RIPA buffer (Pierce 89901) containing Halt protease and phosphatase inhibitors (Thermo Scientific) using Qiagen Tissue Lyser II. Protein content was determined by micro bicinchoninic acid protein assay kit (Thermo Scientific). Protein (17 μg) was electrophoresed in 4–20% Mini-Protean TGX precast gels (Bio-Rad, Laboratories, Inc., Hercules, California), then transferred to polyvinylidene difluoride membranes (Bio-Rad). Membranes were blocked with 5% fat-free milk (or 5% bovine serum albumin) in TBS-0.1% Tween and then incubated with appropriate antibodies (Supplementary Table S3). Immunoblots were developed using a SuperSignal West Pico or Femto Chemiluminescence Kit (Thermo Scientific). Density of bands on membranes was analyzed using Image Lab software (Bio-Rad). Approximate size of specific bands was normalized to α-tubulin loaded in the same gel.

Statistical Analyses.

Data are presented as means ± standard deviations (SD). Comparisons between groups were conducted using 2-way ANOVA with Bonferroni post-tests for time-course studies or Student's unpaired *t*-tests for endpoint analyses. All analyses were performed using Prism 6 (GraphPad Software, La Jolla, California).

RESULTS

Obese WT mice lose weight after switching to MR

Our data showed that male obese WT DIO-MR mice lost 45% of their body weight and WT DIO-CF gained 8% 8 weeks after diet initiation (Figure 1A and Table 1), while food intake remained similar throughout the experiment (Figure 1B). EE during light and dark cycles was higher in WT DIO-MR mice compared to controls (Figure 1C) while respiratory quotient (RQ) for both cycles in both groups remained similar (Figure 1D). Whole-body fat and lean masses were reduced in WT DIO-MR mice compared to WT DIO-CF (Figure 1E). pgWAT, iWAT, and BAT masses and their ratios to body weight were lower in WT DIO-MR mice than in controls (Table 1 and Figure 1F). Multilocular beige adipocytes were observed in iWAT of WT DIO-MR mice with upregulated *Ucp1*, *Cidea*, *Tmem26*, *P2rx5*, and *Cox8b* genes, but not in WT DIO-CF (Figure 1G, Supplementary Figure S2A). pgWAT adipocyte sizes were smaller in WT DIO-MR mice than in controls (Supplementary Figure S4A). WT DIO-MR mice had lower circulating TG and TC with higher BHB concentrations compared to WT DIO-CF (Table 2). Additionally, WT DIO-MR mice exhibited lower glucose and insulin concentrations than controls. Furthermore, circulating ADIPOQ and FGF21 were elevated by 1.3- and 20-fold, respectively, in WT DIO-MR mice, while leptin and IGF-1 were lower compared to WT DIO-CF mice (Table 2).

Weight loss in obese mice occurs following a switch to MR even in the absence of ADIPOQ and FGF21

Next, we examined the roles of ADIPOQ and FGF21 during weight loss in DIO-MR mice by using mice that are deficient in either *Adipoq* or *Fgf21*. Additionally, to exclude the possibility of compensation by one hormone in the absence of the other hormone, we created mice that have simultaneous deletion of both hormones —*Adipoq*/*Fgf21*-KO double-knockouts (AF-dKO DIO)—and induced obesity. Our data indicate that male *Adipoq*-KO DIO-MR mice lost 36% body weight while *Adipoq*-KO DIO-CF gained 11% (Figure 2A and Table 1). Male *Fgf21*-KO DIO-MR mice lost 40% body weight while *Fgf21*-KO DIO-CF gained 3% (Figure 2B and Table 1). Male AF-dKO DIO-MR mice lost 38% body weight while AF-dKO DIO-CF gained (Figure 2C and Table 1). Food intake remained similar between male DIO-CF and -MR mice from each cohort (Figure 2D–2F). pgWAT, iWAT, and BAT masses and their ratio to body weight in all cohorts of male DIO-MR mice were lower than DIO-CF mice (Figure 2G–2I and Table 1). Additionally, female *FGF21*-KO and AF-dKO DIO-MR mice also experienced weight loss (Supplementary Table S4, Supplementary Figure S1A and S1C, respectively) and correspondingly smaller pgWAT, iWAT, and BAT depots (Supplementary Table S4, Supplementary Figure S1B–S1D, respectively) compared to female control counterparts. pgWAT adipocytes were smaller in all genotypes of male DIO-MR mice than in DIO-CF mice (Supplementary Figure S4B–S4D). Multilocular

adipocytes, which were confirmed to be beige adipose tissue due to upregulated *Ucp1*, *Pgc1a*, *Cidea*, *Tmem26*, and *Cox8b* genes (Supplementary Figure S2C and S2D), were observed in iWAT of male *Adipoq*-KO DIO-MR but not in *Adipoq*-KO DIO-CF mice (Figure 2J). iWAT from male *Fgf21*-KO and AF-dKO DIO-MR mice did not exhibit multilocular adipocytes or beige adipose tissue gene expression profile compared to their respective controls (Figure 2J, Supplementary Figure S2E–S2H).

Male *Adipoq*- and/or *Fgf21*-KO DIO-MR exhibited a metabolically healthy circulating profile (Table 2) compared to their control counterparts. *Adipoq*-KO, *Fgf21*-KO, and AF-dKO DIO-MR mice had lower glucose, TC, insulin, leptin, and IGF-1 concentrations compared to their respective controls. Plasma TG concentrations were lower in *Adipoq*-KO and AF-dKO DIO-MR mice compared to their respective controls, but were unchanged in both groups of *Fgf21*-KO DIO mice. Circulating BHB was elevated in AF-dKO DIO-MR mice compared to AF-dKO DIO-CF but remained similar in both groups of *Adipoq*-KO and *Fgf21*-KO DIO mice. Circulating FGF21 concentrations were 30-fold higher in *Adipoq*-KO DIO-MR mice compared to *Adipoq*-KO DIO-CF mice, whereas ADIPOQ levels were 50% higher in *Fgf21*-KO DIO-MR mice compared to *Fgf21*-KO DIO-CF mice. As expected, circulating ADIPOQ and FGF21 were not detected in *Adipoq*-KO and *Fgf21*-KO mice respectively, or in AF-dKO mice.

Reduced adipose tissue mass during MR is due to increased lipolysis and changes in hormone-regulated lipogenesis

Next, we examined whether weight loss in DIO-MR mice involves a futile lipid cycle in adipose tissue, as described previously (3). We measured protein and gene expressions from iWAT and pgWAT of male WT and AF-dKO mice. Our data indicate that ATGL, a lipolytic enzyme, was upregulated in iWAT and pgWAT of WT and AF-dKO DIO-MR mice compared to their respective controls (Figure 3 and Supplementary Figure S3). Levels of fatty acid synthase (FASN), a lipogenic enzyme, showed no differences in iWAT and pgWAT from WT- and AF-dKO mice, but they were upregulated in pgWAT of WT DIO-MR mice and downregulated in both depots of *Fgf21*-KO and AF-dKO DIO-MR mice compared to controls (Figure 3 and Supplementary Figure S3). The expression of the lipogenic enzyme stearoyl-CoA desaturase (SCD1) was upregulated in WT- and *Adipoq*-KO DIO-MR mice but downregulated in *Fgf21*-KO and AF-dKO DIO-MR mice compared to control counterparts (Figure 3 and Supplementary Figure S3).

Reduced adipose tissue mass during MR is due to depot-specific changes in apoptosis

Next, we examined whether adipocyte apoptosis is involved in reducing fat mass during MR. Studies in rats have demonstrated that a leptin mediated reduction in fat mass occurs in concert with activation of adipocyte apoptosis (23). Additionally, MR-activated apoptosis was shown to reduce tumor size in a mouse breast cancer model (24). Thus, we examined whether MR-induced apoptosis in fat corresponds to reduced adipose tissue mass. Our data indicate that protein expression of cleaved apoptosis-inducible factor AIF (57 kDa), non-caspase-dependent apoptosis, was increased in pgWAT of male WT DIO-MR mice compared to WT DIO-CF (Figure 4C) but not in iWAT (Figure 4A). Expression levels of total AIF (67 kDa), but not its cleaved form, were also increased in iWAT and pgWAT of

AF-dKO DIO MR mice compared to control counterparts (Figure 4B and 4D). Interestingly, we did not observe changes in protein expression of caspase 3 in iWAT and pgWAT from WT and AF-dKO DIO mice.

MR induces an adipose tissue depot-specific autophagic response

Based on current data, our findings suggest distinct regulation of adipose tissue mass during MR in different depots, which prompted us to investigate other regulators of adipose tissue homeostasis. One such regulator is autophagy (25,26). Importantly, in yeast, the lifespan extension benefit by MR is associated with autophagy (27); thus, we examined the link between MR and autophagy on adipose tissue homeostasis in male DIO mice. We found an adipose tissue depot-specific effect of MR in autophagy-related protein expression that is independent of ADIPOQ and FGF21. iWAT from WT and AF-dKO DIO-MR mice showed increased levels for chaperone-mediated autophagy (CMA) proteins such as lysosomal-associated membrane proteins 1 and 2 (LAMP1 and LAMP2) compared to their DIO-CF groups while expression for macroautophagy proteins such as autophagy-related proteins 5 and 7 (ATG5 and ATG7), Beclin1, light chain 3 BI, and BII (LC3BI and LC3BII) remained similar in all groups (Figures 5A and 5B). Additionally, the ratios of LC3BII to LC3BI are lower in iWAT of WT and AF-dKO DIO-MR mice compared to controls (Figure 5C). On the other hand, pgWAT from WT and AF-dKO DIO-MR mice showed increased expression of macroautophagy proteins compared to their DIO-CF counterparts, while CMA protein levels remained similar in all groups (Figures 5D and 5E). The ratios of LC3BII to LC3BI were unchanged in both groups (Figure 5F).

MR improves glucose metabolism even in the absence of ADIPOQ and FGF21

Next, we asked whether weight loss during MR also affected peripheral tissues by examining glucose metabolism in obese mice. Our data indicate that all cohorts of male DIO-MR mice show improved glucose tolerance compared to their DIO-CF counterparts (Figure 6A–6D). Hepatic glucose production was reduced in AF-dKO DIO-MR mice compared to controls as measured by PTT (Figure 6E). Additionally, AF-dKO DIO-MR mice tended to be more insulin sensitive than controls, but these data were not statistically significant (Figure 6F).

DISCUSSION

There are several important results in our study. 1. A high-fat diet that contains reduced levels of methionine promotes weight loss in obese mice. 2. Formation of beige adipose tissue is not necessary during weight loss. 3. Adiponectin and FGF21 are not involved in weight loss during MR. 4. Non-caspase-mediated apoptosis plays a role in reducing fat mass. 5. An adipose tissue depot-specific response during MR promotes CMA in iWAT and macroautophagy in pgWAT. The use of obese mice before switching to the DIO-CF or DIO-MR diets provides a tool to elucidate the effects of MR on adipose tissue homeostasis.

Our data agree with previous reports that weight loss exhibited by DIO-MR mice does not involve ADIPOQ or FGF21 (17,28). However, those studies did not show involvement of either FGF21 in *Adipoq*-KO or ADIPOQ in *Fgf21*-KO MR mice (17,28). Here, we present

data from male and female AF-dKO DIO-MR mice that weight loss during MR does not involve ADIPOQ and FGF21. Additionally, despite reports that show ADIPOQ and FGF21 can independently induce weight loss (12,13), their actions may complement each other. For example, mice overexpressing FGF21 increase serum adiponectin and do not gain weight after HFD feeding (18,29). Also, *Fgf21*-KO mice exhibit significantly lower serum adiponectin levels under lean and DIO conditions (18,19). Our data suggest that MR acts on regulators that are upstream of ADIPOQ and FGF21 to induce weight loss.

Histomorphology and gene expression analyses show that WT- and *Adipoq*-KO DIO-MR mice exhibit beige adipose tissue formation but *Fgf21*-KO and AF-dKO DIO-MR mice do not. However, circulating biomarkers of all DIO-MR cohorts show lower lipid levels and an insulin-sensitive profile with improved glucose tolerance compared to controls. Beige adipocytes have been shown to protect against obesity and development of insulin resistance (30). In this context, beige adipose tissue in MR mice expressing UCP1 protein with enhanced mitochondrial biogenesis has been demonstrated (20). Our data regarding WT and *Adipoq*-KO DIO-MR mice agree with previous studies implicating FGF21 in beige adipose tissue formation, which confers protection from obesity and diabetes during MR (16). However, data from *Fgf21*-KO and AF-dKO mice do not fully explain weight loss, reduced fat mass, and healthy circulating profile during MR as being a result of increased beige cell development and UCP1-mediated thermogenesis. Thus, our data suggest that weight loss during MR promotes a metabolically healthy profile regardless of the appearance of beige fat and actions of FGF21.

While increased lipolysis and lipogenesis in WT DIO-MR mice is consistent with previous studies using MR rats (3), increased lipolysis but reduced lipogenesis markers are observed in AF-dKO DIO-MR mice, suggesting that a futile lipid cycle is driven by actions of ADIPOQ and FGF21. Thus, during MR in the absence of ADIPOQ and FGF21 hormones, lipolysis is favored while lipogenesis is dampened to reduce fat accumulation. This suggests that MR will reduce adiposity regardless of actions of other proteins responsible for energy balance. In fact, MR in mice deficient in SCD1 (a lipogenic enzyme), protein tyrosine phosphatase 1B (PTP1B, a negative regulator of insulin signaling), or general control nonderepressible 2 (GCN2, an amino acid sensing kinase) also reduced body weight gain and fat accumulation (31–33). Thus, alternate mechanisms influence the actions of MR to reduce fat mass.

A potential mechanism involved in reducing fat mass during MR is apoptosis. Adipose tissue apoptosis contributes to obesity-related complications in mice (34). Additionally, obesity-related macrophage-secreted factors induce insulin resistance and apoptosis of adipocytes (35). On the other hand, MR activates caspase-induced apoptosis to reduce the size of tumors in a breast cancer mouse model (24). We found that non-caspase-mediated apoptosis is modestly increased only in pgWAT of WT DIO-MR and not in iWAT. Our data demonstrate that MR induces adipose tissue apoptosis under obese conditions, which may contribute to reduction of fat mass and promote insulin sensitivity.

Lipophagy, elimination of lipid droplets through autophagic pathway, may provide a mechanism that could reduce fat mass during MR (36,37). Inhibition of autophagy in mouse

hepatocytes leads to accumulation of lipids, which is accompanied by decreased lipolysis (36). In line with this, our data reveal that MR upregulates lipolysis as well as autophagy-related proteins in an adipose tissue depot-specific response in WT and AF-dKO DIO mice. An adipose tissue depot-specific effect on autophagy was demonstrated in Wistar Ottawa Karlsburg W rats, a model for metabolic syndrome, where iWAT shows an increase in LC3-II/LC3-I ratio while pgWAT exhibits upregulated ATG5 and ATG7 proteins (38). Our data in iWAT indicate that CMA (LAMP1 and LAMP2) is upregulated during MR. Previous studies show that CMA blockage lead to hepatic lipid droplet accumulation (39). Furthermore, CMA has been shown to precede lipolysis by degrading lipid droplet-associated proteins such as perilipins 2 and 3 (26). It is, therefore, possible that reduced iWAT mass in DIO-MR is due to upregulated CMA and increased lipolysis. In parallel, reduced pgWAT mass could primarily be due to increased lipolysis associated with upregulated macroautophagy (LC3B) instead of CMA activation. Our data is consistent with a study showing that an increase in LC3 in muscle leads to removal of lipids (37). Interestingly, reduction of TG in myocytes was shown to be independent of lipolysis, suggesting that autophagy and other mechanisms promote TG removal (37). Our data uncover a depot-specific upregulation of autophagy during MR that could lead to smaller fat size.

We also demonstrate peripheral benefits of MR with improved glucose metabolism in DIO mice independent of the actions of ADIPOQ and FGF21. Our data agree with a recent report that showed FGF21 is not involved in reducing hepatic and adipose tissue inflammation during MR (28). Interestingly, iWAT and skeletal muscle from *Fgf21*-KO MR mice were more insulin sensitive than *Fgf21*-KO CF, albeit less sensitive than WT counterparts (16). Finally, improvements in glucose metabolism during MR is independent of ADIPOQ (17). Thus, we propose that other factors besides ADIPOQ and FGF21 contribute to the benefits of MR.

A limitation of our study is that DIO-MR mice may have adapted to conditions following weight loss and maintained a steady state. Thus, short-term longitudinal diet experiments would provide a more detailed physiological mechanism as weight loss progresses. Another limitation is that our data showed changes specific only to iWAT and pgWAT. It would be worthwhile to examine molecular changes in other fat depots, such as perivascular adipose tissue, in response to weight loss.

In summary, our study has uncovered a coordinated adaptive response during weight loss in DIO-MR mice that involves lipolysis, lipogenesis, apoptosis, and autophagy but does not involve ADIPOQ or FGF21. Mechanistically, besides increasing lipolysis, our data suggest that MR induces weight loss via an adipose tissue depot-specific non-caspase-mediated apoptosis concomitant with activation of autophagosome formation in pgWAT, and CMA in iWAT in DIO mice. Given that an MR diet primarily consists of plant-based food sources rather than animal-based food sources (40), implementing an MR diet could be an effective weight loss regimen for obese human subjects.

Supplementary Material

Refer to Web version on PubMed Central for supplementary material.

ACKNOWLEDGEMENTS

The authors would like to thank Angela Tremain (OFAS) and Dr. Arthur Cooper (New York Medical College) for help in editing.

FUNDING: This work was supported by the Orentreich Foundation for the Advancement of Science, Inc. ASL13, ASL22 and ASL24, and utilized the services of the MMCRI Physiology Core supported by NIH/NIGMS P30GM106391, P20GM121301 and U54GM115516.

References

1. Massetti GM, Dietz WH, and Richardson LC (2017) Excessive Weight Gain, Obesity, and Cancer: Opportunities for Clinical Intervention. JAMA 318, 1975–1976 [PubMed: 28973170]
2. Upadhyay J, Farr O, Perakakis N, Ghaly W, and Mantzoros C (2018) Obesity as a Disease. Med Clin North Am 102, 13–33 [PubMed: 29156181]
3. Perrone CE, Mattocks DA, Hristopoulos G, Plummer JD, Krajcik RA, and Orentreich N (2008) Methionine restriction effects on 11 -HSD1 activity and lipogenic/lipolytic balance in F344 rat adipose tissue. J Lipid Res 49, 12–23 [PubMed: 17909224]
4. Castano-Martinez T, Schumacher F, Schumacher S, Kochlik B, Weber D, Grune T, Biemann R, McCann A, Abraham K, Weikert C, Kleuser B, Schurmann A, and Laeger T (2019) Methionine restriction prevents onset of type 2 diabetes in NZO mice. FASEB J, fj201900150R
5. Forney LA, Wanders D, Stone KP, Pierse A, and Gettys TW (2017) Concentration-dependent linkage of dietary methionine restriction to the components of its metabolic phenotype. Obesity (Silver Spring) 25, 730–738 [PubMed: 28261952]
6. Ables GP, Perrone CE, Orentreich D, and Orentreich N (2012) Methionine-restricted C57BL/6J mice are resistant to diet-induced obesity and insulin resistance but have low bone density. PLoS One 7, e51357 [PubMed: 23236485]
7. Yamauchi T, Kamon J, Waki H, Terauchi Y, Kubota N, Hara K, Mori Y, Ide T, Murakami K, Tsuboyama-Kasaoka N, Ezaki O, Akanuma Y, Gavrilova O, Vinson C, Reitman ML, Kagechika H, Shudo K, Yoda M, Nakano Y, Tobe K, Nagai R, Kimura S, Tomita M, Froguel P, and Kadowaki T (2001) The fat-derived hormone adiponectin reverses insulin resistance associated with both lipoatrophy and obesity. Nat Med 7, 941–946 [PubMed: 11479627]
8. Kharitonenkov A, Shiyanova TL, Koester A, Ford AM, Micanovic R, Galbreath EJ, Sandusky GE, Hammond LJ, Moyers JS, Owens RA, Gromada J, Brozinick JT, Hawkins ED, Wroblewski VJ, Li DS, Mehrbod F, Jaskunas SR, and Shanafelt AB (2005) FGF-21 as a novel metabolic regulator. J Clin Invest 115, 1627–1635 [PubMed: 15902306]
9. Kliewer SA, and Mangelsdorf DJ (2019) A Dozen Years of Discovery: Insights into the Physiology and Pharmacology of FGF21. Cell Metab 29, 246–253 [PubMed: 30726758]
10. Iwabu M, Okada-Iwabu M, Yamauchi T, and Kadowaki T (2015) Adiponectin/adiponectin receptor in disease and aging. NPJ Aging Mech Dis 1, 15013 [PubMed: 28721260]
11. Xu J, Stanislaus S, Chinookoswong N, Lau YY, Hager T, Patel J, Ge H, Weiszmann J, Lu SC, Graham M, Busby J, Hecht R, Li YS, Li Y, Lindberg R, and Veniant MM (2009) Acute glucose-lowering and insulin-sensitizing action of FGF21 in insulin-resistant mouse models--association with liver and adipose tissue effects. Am J Physiol Endocrinol Metab 297, E1105–1114 [PubMed: 19706786]
12. Qi Y, Takahashi N, Hileman SM, Patel HR, Berg AH, Pajvani UB, Scherer PE, and Ahima RS (2004) Adiponectin acts in the brain to decrease body weight. Nat Med 10, 524–529 [PubMed: 15077108]
13. Owen BM, Ding X, Morgan DA, Coate KC, Bookout AL, Rahmouni K, Kliewer SA, and Mangelsdorf DJ (2014) FGF21 acts centrally to induce sympathetic nerve activity, energy expenditure, and weight loss. Cell Metab 20, 670–677 [PubMed: 25130400]
14. Fisher FM, Kleiner S, Douris N, Fox EC, Mepani RJ, Verdeguer F, Wu J, Kharitonenkov A, Flier JS, Maratos-Flier E, and Spiegelman BM (2012) FGF21 regulates PGC-1alpha and browning of white adipose tissues in adaptive thermogenesis. Genes Dev 26, 271–281 [PubMed: 22302939]

15. Wei Q, Lee JH, Wang H, Bongmba OYN, Wu CS, Pradhan G, Sun Z, Chew L, Bajaj M, Chan L, Chapkin RS, Chen MH, and Sun Y (2017) Adiponectin is required for maintaining normal body temperature in a cold environment. BMC Physiol 17, 8 [PubMed: 29058611]
16. Wanders D, Forney LA, Stone KP, Burk DH, Pierse A, and Gettys TW (2017) FGF21 Mediates the Thermogenic and Insulin-Sensitizing Effects of Dietary Methionine Restriction but Not Its Effects on Hepatic Lipid Metabolism. Diabetes 66, 858–867 [PubMed: 28096260]
17. Stone KP, Wanders D, Calderon LF, Spurgin SB, Scherer PE, and Gettys TW (2015) Compromised responses to dietary methionine restriction in adipose tissue but not liver of ob/ob mice. Obesity (Silver Spring) 23, 1836–1844 [PubMed: 26237535]
18. Holland WL, Adams AC, Brozinick JT, Bui HH, Miyauchi Y, Kusminski CM, Bauer SM, Wade M, Singhal E, Cheng CC, Volk K, Kuo MS, Gordillo R, Kharitonenkov A, and Scherer PE (2013) An FGF21-adiponectin-ceramide axis controls energy expenditure and insulin action in mice. Cell Metab 17, 790–797 [PubMed: 23663742]
19. Lin Z, Tian H, Lam KS, Lin S, Hoo RC, Konishi M, Itoh N, Wang Y, Bornstein SR, Xu A, and Li X (2013) Adiponectin mediates the metabolic effects of FGF21 on glucose homeostasis and insulin sensitivity in mice. Cell Metab 17, 779–789 [PubMed: 23663741]
20. Patil YN, Dille KN, Burk DH, Cortez CC, and Gettys TW (2015) Cellular and molecular remodeling of inguinal adipose tissue mitochondria by dietary methionine restriction. J Nutr Biochem 26, 1235–1247 [PubMed: 26278039]
21. Potthoff MJ, Inagaki T, Satapati S, Ding X, He T, Goetz R, Mohammadi M, Finck BN, Mangelsdorf DJ, Kliewer SA, and Burgess SC (2009) FGF21 induces PGC-1alpha and regulates carbohydrate and fatty acid metabolism during the adaptive starvation response. Proc Natl Acad Sci U S A 106, 10853–10858 [PubMed: 19541642]
22. Ma K, Cabrero A, Saha PK, Kojima H, Li L, Chang BH, Paul A, and Chan L (2002) Increased beta -oxidation but no insulin resistance or glucose intolerance in mice lacking adiponectin. J Biol Chem 277, 34658–34661 [PubMed: 12151381]
23. Qian H, Azain MJ, Compton MM, Hartzell DL, Hausman GJ, and Baile CA (1998) Brain administration of leptin causes deletion of adipocytes by apoptosis. Endocrinology 139, 791–794 [PubMed: 9449655]
24. Hens JR, Sinha I, Perodin F, Cooper T, Sinha R, Plummer J, Perrone CE, and Orentreich D (2016) Methionine-restricted diet inhibits growth of MCF10AT1-derived mammary tumors by increasing cell cycle inhibitors in athymic nude mice. BMC Cancer 16, 349 [PubMed: 27255182]
25. Zhang Y, Goldman S, Baerga R, Zhao Y, Komatsu M, and Jin S (2009) Adipose-specific deletion of autophagy-related gene 7 (atg7) in mice reveals a role in adipogenesis. Proc Natl Acad Sci U S A 106, 19860–19865 [PubMed: 19910529]
26. Kaushik S, and Cuervo AM (2015) Degradation of lipid droplet-associated proteins by chaperone-mediated autophagy facilitates lipolysis. Nat Cell Biol 17, 759–770 [PubMed: 25961502]
27. Ruckenstuhl C, Netzberger C, Entfellner I, Carmona-Gutierrez D, Kickenweiz T, Stekovic S, Gleixner C, Schmid C, Klug L, Sorgo AG, Eisenberg T, Buttner S, Marino G, Koziel R, Jansen-Durr P, Frohlich KU, Kroemer G, and Madeo F (2014) Lifespan extension by methionine restriction requires autophagy-dependent vacuolar acidification. PLoS Genet 10, e1004347 [PubMed: 24785424]
28. Sharma S, Dixon T, Jung S, Graff EC, Forney LA, Gettys TW, and Wanders D (2019) Dietary Methionine Restriction Reduces Inflammation Independent of FGF21 Action. Obesity (Silver Spring)
29. Ding X, Boney-Montoya J, Owen BM, Bookout AL, Coate KC, Mangelsdorf DJ, and Kliewer SA (2012) betaKlotho is required for fibroblast growth factor 21 effects on growth and metabolism. Cell Metab 16, 387–393 [PubMed: 22958921]
30. Kajimura S, Spiegelman BM, and Seale P (2015) Brown and Beige Fat: Physiological Roles beyond Heat Generation. Cell Metab 22, 546–559 [PubMed: 26445512]
31. Forney LA, Stone KP, Wanders D, Ntambi JM, and Gettys TW (2018) The role of suppression of hepatic SCD1 expression in the metabolic effects of dietary methionine restriction. Appl Physiol Nutr Metab 43, 123–130 [PubMed: 28982014]

32. Lees EK, Krol E, Shearer K, Mody N, Gettys TW, and Delibegovic M (2015) Effects of hepatic protein tyrosine phosphatase 1B and methionine restriction on hepatic and whole-body glucose and lipid metabolism in mice. Metabolism 64, 305–314 [PubMed: 25468142]
33. Wanders D, Stone KP, Forney LA, Cortez CC, Dille KN, Simon J, Xu M, Hotard EC, Nikonorova IA, Pettit AP, Anthony TG, and Gettys TW (2016) Role of GCN2-Independent Signaling Through a Noncanonical PERK/NRF2 Pathway in the Physiological Responses to Dietary Methionine Restriction. Diabetes 65, 1499–1510 [PubMed: 26936965]
34. Alkhouri N, Gornicka A, Berk MP, Thapaliya S, Dixon LJ, Kashyap S, Schauer PR, and Feldstein AE (2010) Adipocyte apoptosis, a link between obesity, insulin resistance, and hepatic steatosis. J Biol Chem 285, 3428–3438 [PubMed: 19940134]
35. Keuper M, Bluher M, Schon MR, Moller P, Dzyakanchuk A, Amrein K, Debatin KM, Wabitsch M, and Fischer-Posovszky P (2011) An inflammatory micro-environment promotes human adipocyte apoptosis. Mol Cell Endocrinol 339, 105–113 [PubMed: 21501656]
36. Singh R, Kaushik S, Wang Y, Xiang Y, Novak I, Komatsu M, Tanaka K, Cuervo AM, and Czaja MJ (2009) Autophagy regulates lipid metabolism. Nature 458, 1131–1135 [PubMed: 19339967]
37. Lam T, Harmancey R, Vasquez H, Gilbert B, Patel N, Hariharan V, Lee A, Covey M, and Taegtmeyer H (2016) Reversal of intramyocellular lipid accumulation by lipophagy and a p62-mediated pathway. Cell Death Discov 2, 16061 [PubMed: 27625792]
38. Kosacka J, Koch K, Gericke M, Nowicki M, Heiker JT, Kloting I, Stumvoll M, Bluher M, and Kloting N (2013) The polygenetically inherited metabolic syndrome of male WOKW rats is associated with enhanced autophagy in adipose tissue. Diabetol Metab Syndr 5, 23 [PubMed: 23668414]
39. Schneider JL, Villarroya J, Diaz-Carretero A, Patel B, Urbanska AM, Thi MM, Villarroya F, Santambrogio L, and Cuervo AM (2015) Loss of hepatic chaperone-mediated autophagy accelerates proteostasis failure in aging. Aging Cell 14, 249–264 [PubMed: 25620427]
40. Ables GP, and Johnson JE (2017) Pleiotropic responses to methionine restriction. Exp Gerontol 94, 83–88 [PubMed: 28108330]

What is already known about this subject?

- MR prevents obesity due to a futile lipid cycle.
- Beige adipose tissue formation is indicative of a healthy metabolic status.
- Circulating adiponectin and FGF21 are consistently elevated during MR.

What does your study add?

- MR promotes weight loss not just by a futile lipid cycle, but also by a coordinated response that involves apoptosis and autophagy to maintain homeostasis.
- Adiponectin and FGF21 are not essential to reduce adiposity during MR.
- Adipose tissue depot-specific response to maintain homeostasis is activated during MR in response to weight loss.

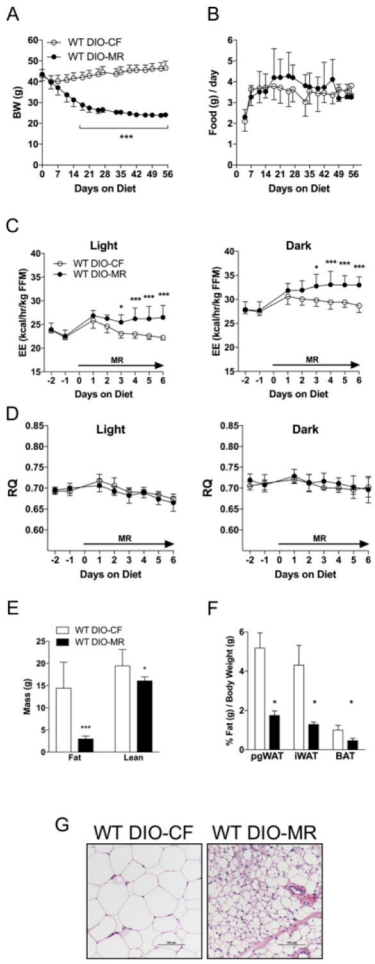

Figure 1.

Male obese WT mice lose weight after switching to an MR diet. (**A**) Body weight and (**B**) daily food consumption of WT DIO-CF (open circles) and WT DIO-MR (filled circles) mice following 8 weeks of HFD feeding. (**C**) Energy expenditure (EE) and (**D**) respiratory quotient (RQ) WT DIO-CF and -MR mice. Data are normalized to fat-free mass (FFM). (**E**) Whole-body fat and lean masses WT DIO-CF (white bars) and -MR (black bars) mice. (**F**) Perigonadal (pgWAT), inguinal (iWAT), and brown AT (BAT) sizes relative to body weight in WT DIO-CF and -MR mice. (**G**) Appearance of multilocular adipocytes in iWAT of WT DIO-MR mice but not in DIO-CF mice. Scale bar denotes 100 μm. Statistical analysis was conducted using 2-way ANOVA for time-course experiments (A - D) or Student's *t*-test for end-point experiments (E and F), as described in Methods (n = 7 – 8 / group, ***P < 0.001, *P < 0.05).

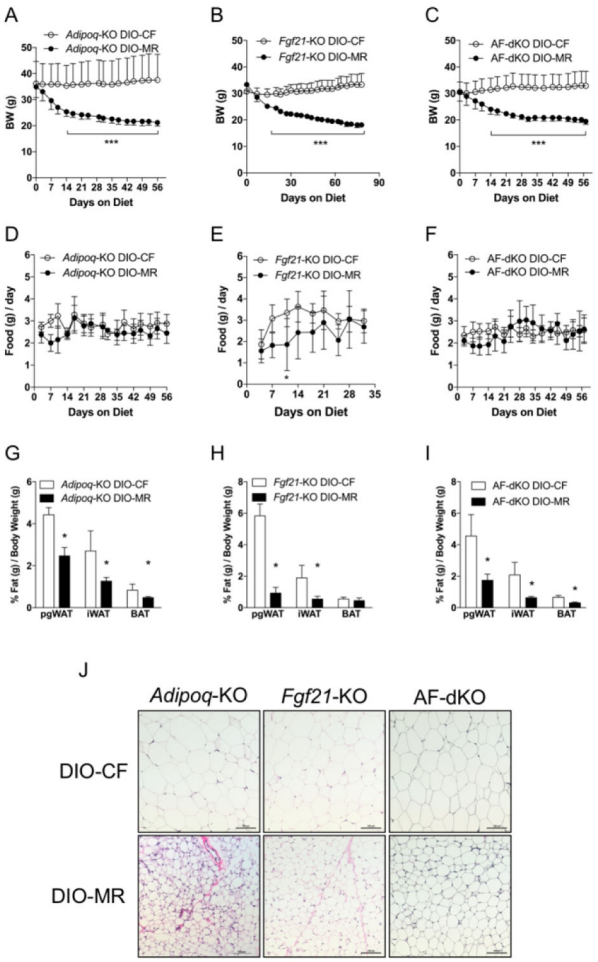

Figure 2.

Weight loss in male obese mice occurs following a switch to MR in the absence of ADIPOQ and FGF21. (**A - C**) Body weights and (**D - F**) daily food consumption of *Adipoq*-KO DIO-CF, *Fgf21*-KO DIO-CF, and AF-dKO DIO-CF (open circles) and -MR mice (filled circles). (**G - I**) The ratios of perigonadal (pgWAT), inguinal (iWAT), and intrascapular BAT masses relative to body weight in *Adipoq*-KO DIO-CF, *Fgf21*-KO DIO-CF, and AF-dKO DIO-CF (white bars) and -MR (black bars) mice. (**J**) H & E staining of iWAT from *Adipoq*-KO (left panels), *Fgf21*-KO (middle panels), and AF-dKO (right panels) DIO-CF (Top panels) and -MR (Bottom panels) mice. Scale bar denotes 100μm. Statistical analysis was conducted using 2-way ANOVA for time-course experiments (A - F) or Student's *t*-test between CF and MR for each adipose tissue depot (G - I), as described in Methods (n = 7 – 8 / group, ***P < 0.001, *P < 0.05).

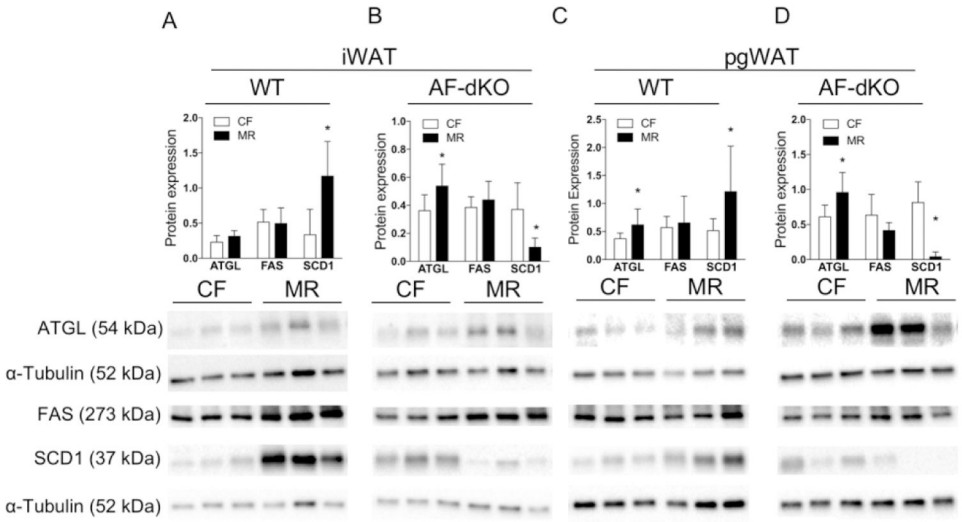

Figure 3.

Reduced fat mass in male obese mice during MR, lipolysis and hormone-regulated lipogenesis. Protein expression of ATGL, FAS and SCD1, normalized to α-tubulin and respective immunoblots in iWAT (**A** and **B**) and pgWAT (**C** and **D**) of WT DIO (**A** and **C**) and AF-dKO (**B** and **D**) mice fed CF (white bars) or MR (black bars). Statistical analysis was conducted using Student's *t*-test between CF and MR in each cohort, as described in Methods (n = 7 – 8 / group, *P < 0.05).

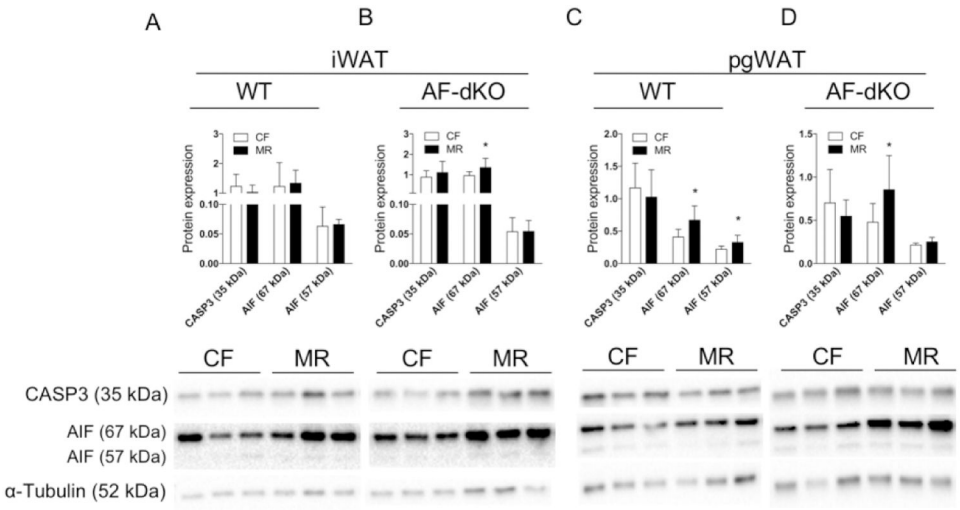

Figure 4.

Reduced fat mass in male obese mice during MR and apoptosis. Protein expression for Caspase 3 (CASP3) and Apoptosis-Inducible Factor (total protein: AIF 67 kDa and cleaved protein AIF 57 kDa) normalized to α-tubulin and their respective immunoblots from iWAT (**A** and **B**) and pgWAT (**C** and **D**) of WT DIO (**A** and **C**) and AF-dKO (**B** and **D**) mice fed either CF (white bars) or MR (black bars). Statistical analysis was conducted using Student's *t*-test for each protein between CF and MR in each cohort, as described in Methods (n = 7 – 8 / group, *P < 0.05).

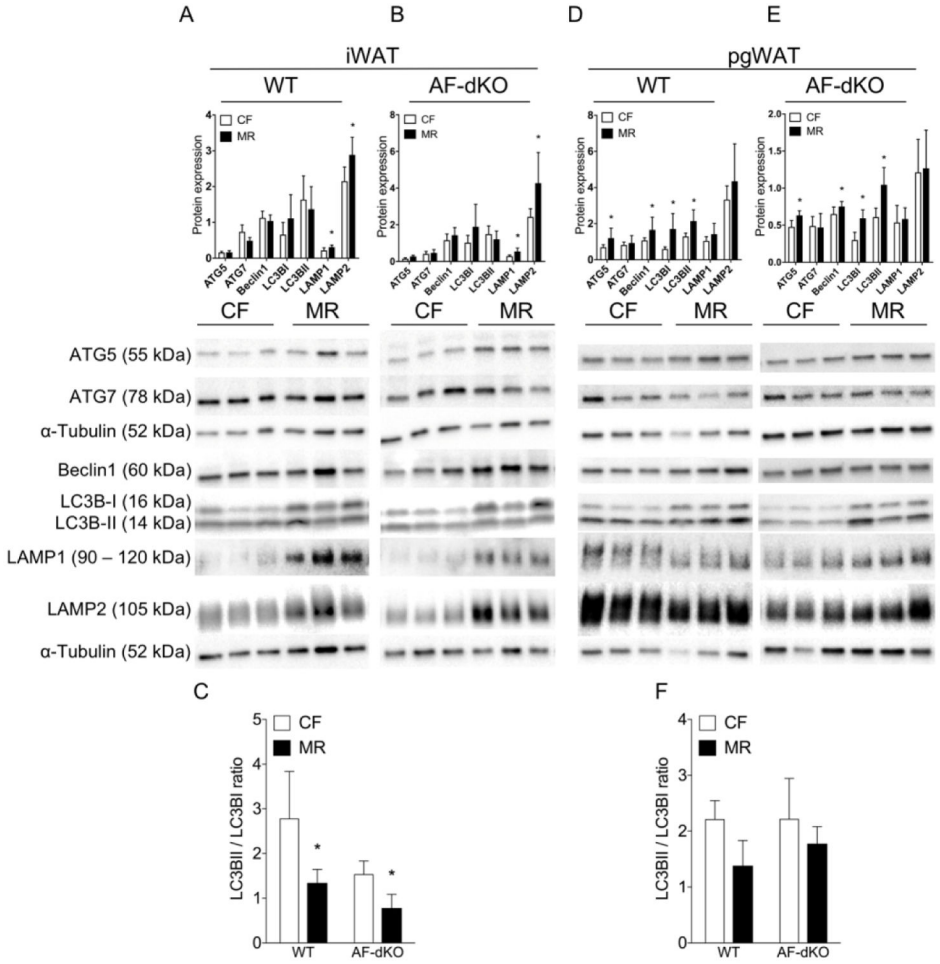

Figure 5.

MR induces an adipose tissue-depot specific autophagic response in male obese mice. Protein expression for ATG5, ATG7, Beclin1, LC3B, LAMP1 and LAMP1 normalized to α-tubulin and their respective immunoblots from iWAT (**A** and **B**) and pgWAT (**D** and **E**) of WT DIO (**A** and **D**) and AF-dKO (**B** and **E**) mice fed either CF (white bars) or MR (black bars). The ratios of LC3BII/I from iWAT of WT DIO (**C**) and pgWAT of AF-dKO (**F**). Statistical analysis was conducted using Student's *t*-test for each protein between CF and MR in each cohort, as described in Methods (n = 7 – 8 / group, *P < 0.05).

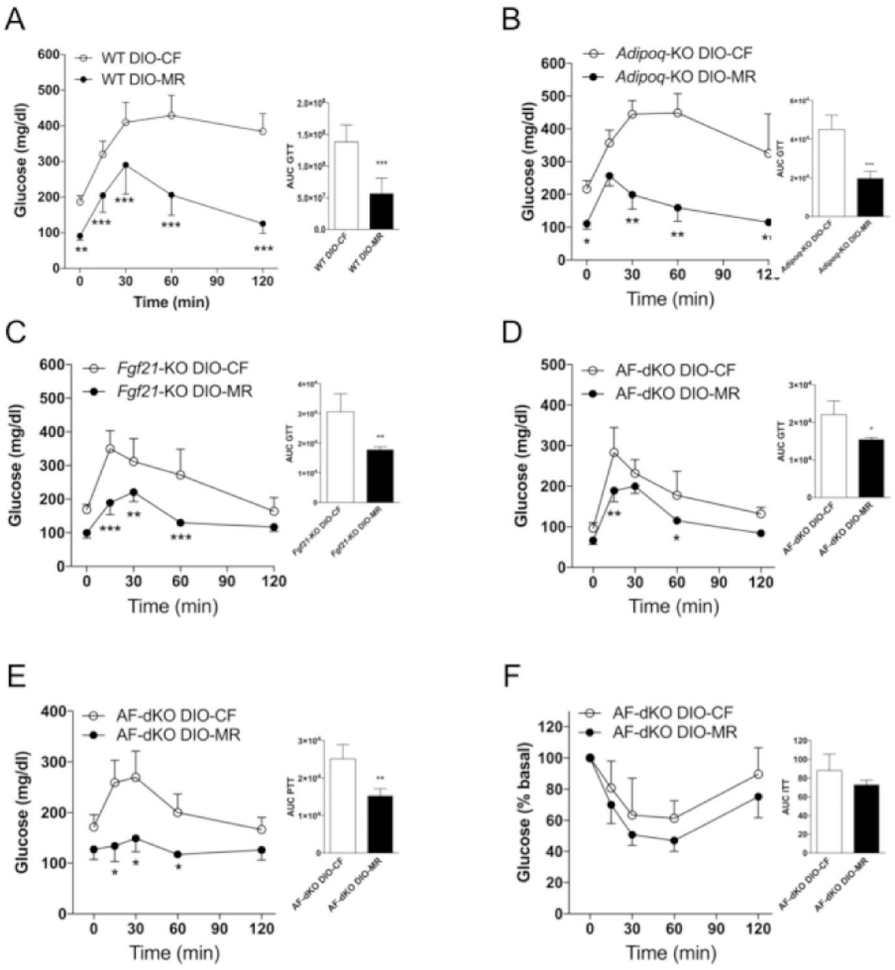

Figure 6.

Weight loss in male obese mice improves glucose tolerance during MR. Glucose tolerance tests were conducted as described in Methods in (**A**) WT, (**B**) Adpn-KO (**C**) FGF21-KO, and (**D**) AF-dKO DIO mice that were fed either a CF or MR diet for 4 weeks. (**E**) Pyruvate and (**F**) insulin tolerance tests in AF-dKO DIO mice were conducted at 5 and 7 weeks, respectively, after diet initiation. Statistical analysis was conducted using 2-way ANOVA for time-course experiments or Student's *t*-test for area under the curve (AUC), as described in Methods (n = 4 – 5 / group, **P < 0.001, *P < 0.05).

Table 1.

Body and adipose tissue masses of male WT DIO mice and mice lacking in adiponectin (*Adipoq*-KO), FGF21 (*Fgf21*-KO), or both (AF-dKO) fed a high fat (DIO) CF or MR diet. Comparisons between CF and MR in each cohort were conducted using Student's unpaired *t*-test (n = 5 – 8 / group, ***P < 0.001, **P < 0.01).

	WT DIO		***Adipoq*-KO DIO**		***Fgf21*-KO DIO**		**AF-dKO DIO**	
Mass (g[a])	**CF**	**MR**	**CF**	**MR**	**CF**	**MR**	**CF**	**MR**
Initial Body Weight	42.9 ± 2.9	43.6 ± 3.1	35.4 ± 6.4	32.7 ± 6.9	30.8 ± 2.3	33.3 ± 2.3	30.6 ± 3.7	30.4 ± 3.2
Final Body Weight	46.6 ± 3.3	24.1 ± 1.0***	39.2 ± 7.7	20.6 ± 1.3***	31.7 ± 3.3	19.8 ± 0.5***	32.9 ± 5.5	19.4 ± 1.1***
Body Weight Change	3.6 ± 2.4	−19.6 ± 2.5***	3.4 ± 3.5	−12.1 ± 3.5***	0.9 ± 1.4	−13.5 ± 2.4***	2.4 ± 2.3	−10.3 ± 2.4***
pgWAT	2.4 ± 0.3	0.42 ± 0.04	1.9 ± 0.4	0.51 ± 0.08	2.0 ± 0.5	0.17 ± 0.06	1.6 ± 0.6	0.34 ± 0.08**
iWAT	2.0 ± 0.5	0.31 ± 0.03***	1.2 ± 0.5	0.25 ± 0.05***	0.6 ± 0.3	0.10 ± 0.02***	0.73 ± 0.3	0.13 ± 0.01**
BAT	0.48 ± 0.1	0.11 ± 0.02***	0.42 ± 0.2	0.10 ± 0.01***	0.20 ± 0.05	0.08 ± 0.02***	0.23 ± 0.06	0.06 ± 0.01***

[a]Values are mean ± SD.

Table 2.

Blood biomarkers of male WT DIO mice and mice deficient in adiponectin (*Adipoq*-KO), FGF21 (*Fgf21*-KO), or both (AF-dKO) fed a high fat (DIO) CF or MR diet for 8 weeks. Comparisons between CF and MR in each cohort were conducted using Student's unpaired t-test (n = 5 – 8 / group, *P < 0.05, **P < 0.01, ***P < 0.001). BHB, β-hydroxybutyrate; IGF-1, insulin-like growth factor-1. nd, not detected.

	WT DIO		***Adipoq*-KO DIO**		***Fgf21*-KO DIO**		**AF-dKO DIO**	
	CF	**MR**	**CF**	**MR**	**CF**	**MR**	**CF**	**MR**
Triglyceride (mg/dl)	63 ± 5	53±8*	59 ±6	34 ± 5***	72 ± 7	65±9	43 ± 5	32 ± 4***
Cholesterol (mg/dl)	128 ± 14	84 ± 4***	162 ± 21	111 ± 7***	138 ± 28	98 ± 13*	144 ± 14	105 ± 17***
BHB (mM)	0.1 ± 0.03	0.16 ± 0.04**	0.18 ± 0.04	0.21 ± 0.05	0.1 ± 0.01	0.08 ± 0.02	0.19 ± 0.02	0.29 ± 0.06*
Glucose (mg/dl)	176 ± 25	96 ± 21***	164 ± 28	84 ± 5***	152 ± 22	77 ± 12***	145±7	64 ± 9***
Insulin (ng/ml)	4.2 ± 1.2	0.5 ± 0.4***	2.0 ± 1.6	0.2 ± 0.2*	2.5 ± 1.3	0.8 ± 0.5*	2.0 ± 1.2	0.4 ± 0.2
Leptin (ng/ml)	93±16	2.4 ± 0.8***	22 ± 13	1.4 ± 0.9*	13 ± 9.1	1.2 ± 0.7*	39 ± 29	1.4 ± 0.6**
IGF-1 (ng/ml)	475 ± 59	194 ± 35***	406 ± 93	158 ± 13***	431 ± 81	190 ± 25***	428 ± 39	194 ± 23***
Adiponectin (μg/ml)	10 ± 1.0	14 ± 1.8**	nd	nd	10 ± 1.9	15 ± 2.9**	nd	nd
FGF21 (ng/ml)	0.15 ± 0.1	3.4 ± 1.5**	0.20 ± 0.13	6.9 ± 4.12**	nd	nd	nd	nd

[a]Values are mean ± SD.